Volume 1 | Number 1 | Jan 2013 | Pages 1–100

PCCP

Physical Chemistry Chemical Physics
www.rsc.org/pccp

ROYAL SOCIETY OF CHEMISTRY

ROYAL SOCIETY OF CHEMISTRY

www.rsc.org/pccp

PCCP

ARTICLE

Excitation wavelength-dependent EPR study on the influence of the conformation of multiporphyrin arrays on triplet state delocalization

Claudia E. Tait,[a,†]* Patrik Neuhaus,[b] Martin D. Peeks,[b] Harry L. Anderson,[b] Christiane R. Timmel[a]*

The optoelectronic properties of conjugated porphyrin arrays render them excellent candidates for use in a variety of molecular electronic devices. Understanding the factors controlling the electron delocalization in these systems is important for further developments in this field. Here, we use transient EPR and ENDOR (Electron Nuclear Double Resonance) to study the extent of electronic delocalization in the photoexcited triplet states of a series of butadiyne-linked porphyrin oligomers. We are able to distinguish between planar and twisted arrangements of adjacent porphyrin units, as the different conformations are preferentially excited at different wavelengths in the visible range. We show that the extent of triplet state delocalization is modulated by the torsional angle between the porphyrins and therefore by the excitation wavelength. These results have implications for the design of supramolecular systems with fine-tuned excitonic interactions and for the control of charge transport.

Introduction

Porphyrin-based materials with extensive π-conjugation are good candidates for components in molecular electronic devices and their charge transport properties have been investigated extensively.[1-11] The design of molecular-scale electronic components tailor-made for specific applications requires a thorough knowledge of the electronic and excitonic transfer properties and understanding of the factors influencing these properties at the molecular level. Control and optimization of the optoelectronic properties by molecular design is of particular interest for the development of magnetoelectronic and spintronic devices.

The electron delocalization in the ground, radical cation and photoexcited triplet states of multiporphyrin arrays with different linkers has been the focus of a large number of optical and magnetic resonance studies. [5, 7, 8, 12-22] We have recently demonstrated that the photoexcited triplet state is completely delocalized in a planar butadiyne-linked porphyrin dimer and that delocalization occurs with a reorientation of the ZFS tensor, which shifts the axis of maximum dipolar coupling from the out-of-plane axis in the monomer to the long axis of the molecule in the dimer, achieving alignment of the principal optical and magnetic axes.[21] We have also shown that while this alignment persists for longer porphyrin oligomers with up to six porphyrin units, the ISC mechanism changes for increasing oligomer lengths, leading to changes in the relative populations of the triplet sublevels.[22] The possibility of

obtaining triplet states with such significantly different properties using the same molecular subunit is intriguing and could be relevant for application as a molecular switch or in the context of spintronics.[23, 24]

In this paper, we investigate the influence of different conformations of the porphyrin backbone in butadiyne-linked zinc porphyrin arrays with two to four repeat units, designated as **P1**, **P2**, **P3** and **P4**, on the extent of triplet state delocalization by excitation wavelength-dependent EPR. Optical studies on the porphyrin dimer, **P2**, have shown that the planar and twisted conformations can be selectively excited. [25, 26] The UV-vis absorption spectrum of the porphyrin dimer is characterized by two types of absorption bands, the Q-band (including $S_0 - S_1$) in the wavelength region from about 550 nm to 800 nm and the B- or Soret band centred at about 450 nm. Previous investigations have shown that different conformations of the porphyrin dimer, characterized by different torsional angles around the butadiyne link, contribute to the absorption spectrum in different wavelength regions, as indicated in Figure 1 A.[26] The low rotation barrier (0.67 kcal/mol based on DFT calculations at the B3LYP/6-31G(d) level of theory)[26, 27] around the central butadiyne link means that at room temperature all conformations will be significantly populated, while upon cooling an increasing planarization of the porphyrin dimer occurs.[27] This planarization is reflected in an increase in intensity at 750 nm, corresponding to the absorption of the planar dimer, and a

decrease in intensity at lower wavelengths, where conformations with larger inter-porphyrin dihedral angles contribute to the spectrum. A peak at 680 nm is still present even at 80 K, at which temperature only the near-planar conformations are populated, and is assigned to the vibrational structure of the principal peak of the planar conformer (750 nm) based on the measurement of the emission spectrum and time-dependent DFT (TD-DFT) calculations.[27] At higher temperatures, this vibrational contribution (680 nm) overlaps with the principal absorptions of twisted conformers. The planar conformation of the porphyrin dimer thus absorbs in the whole wavelength region of the Q-band.

The redshift of the long-axis polarized S_0-S_1 absorption for increasing oligomer lengths is indicative of increased conjugation[4] and the concomitant broadening (see Figure 1 B) suggests the contribution of different twisted conformations towards lower wavelengths, but has, to the best of our knowledge, not been investigated in detail yet.

Results and discussion

Porphyrin dimer

The results of transient EPR and ENDOR measurements performed on **P2** using different excitation wavelengths in the region of the Q-band absorption are shown in Figure 2. The

Figure 1. (A) UV-vis absorption spectra of **P2** recorded at room temperature and at 80 K in MeTHF:pyridine 10:1.[27] The absorption bands in the spectra have been assigned to the planar (0°) and twisted (90°) conformations of the porphyrin dimer according to reference.[26] (B) Normalized UV-vis absorption spectra of **P1**, **P2**, **P3** and **P4** recorded at room temperature in MeTHF:pyridine 10:1.

measurements were performed at 20 K either in a MeTHF:pyridine mixture (glass transition temperature of about 100 K), where almost complete planarization of the porphyrin dimer is known to occur,[27] or in *o*-terphenyl (glass transition temperature of 246 K [28]); in this solvent the UV-vis absorption spectrum at 173–238 K (see Figure S2) resembles that at room temperature indicating the presence of a larger range of conformations. The EPR spectra recorded in MeTHF:pyridine only show small changes as a function of excitation wavelength, but in *o*-terphenyl more significant changes are observed (see Figure 2). In particular, the intensity of the Y transitions increases at wavelengths higher than about 650 nm and reaches a maximum at 740−750 nm, and the X canonical peaks broaden towards the centre of the spectrum with the largest broadening observed at around 640-660 nm. The most significant changes in the EPR spectrum thus occur at the wavelengths attributed to the absorption of the twisted dimer conformation (ca. 600−680 nm). Due to the overlap of the absorption band of the twisted conformation with the vibrational structure of the absorption band attributed to the planar conformation, the two spectra will be superimposed and, based on the small changes observed in the experimental time-resolved EPR spectra it would seem that the spectrum of the planar conformation prevails at all wavelengths. The observed dominance of the planar triplet can be explained by the higher triplet yield for this conformation.[29]

Excitation wavelength-dependent ENDOR measurements were also performed at 379 mT, corresponding to the high-field Z transition for the porphyrin monomer and to the high-field X transition for the porphyrin dimer (see Figure 3). In both cases the corresponding triplet axis is aligned with the out-of-plane direction of the porphyrin due to the reorientation of the ZFS tensor occurring between **P1** and **P2**, which exchanges the ZFS Z and X axes.[21] As expected, no wavelength-dependent changes are observed in the ENDOR spectra of **P2** recorded in MeTHF:pyridine and the peak observed at about −1.6 MHz corresponds to the out-of-plane hyperfine coupling of the H_1 protons (β-protons adjacent to the triple bonds, see inset of Figure 1 A) for a triplet state delocalized over both porphyrin units. In *o*-terphenyl, an identical spectrum is obtained for excitation at 750 nm; however excitation at lower wavelengths leads to significant broadening of the same peak and to the appearance of an additional peak at around −2.9 MHz for excitation in the region from 630–670 nm (see arrow in Figure 2 B). The position of this peak corresponds almost exactly to the ENDOR peak observed at the same field position in the porphyrin monomer (see Figure 3 B), except for a small shift towards the Larmor frequency. The good agreement of this peak with the out-of-plane hyperfine coupling of the H_1 protons in the porphyrin monomer and its appearance at wavelengths corresponding to the absorption of the twisted conformation of the porphyrin dimer indicates localization of the triplet state on a single porphyrin unit. The broadening of the peaks towards larger hyperfine couplings at wavelengths lower than 750 nm can be interpreted in terms of contributions of different intermediate conformations with varying hyperfine couplings.
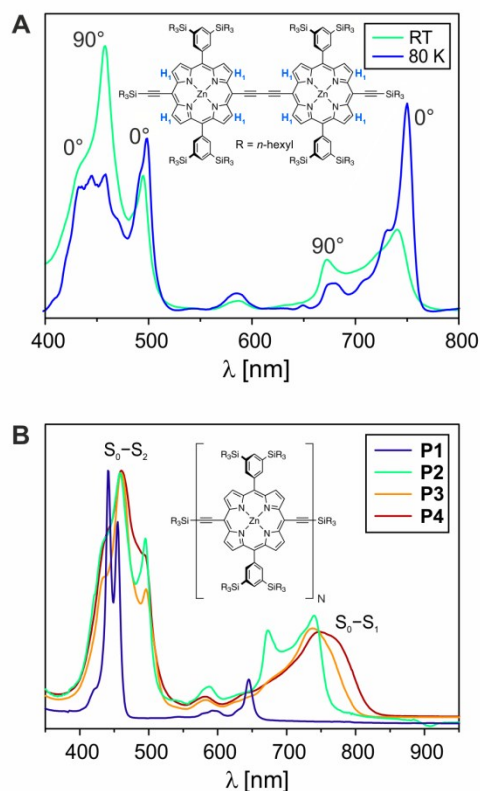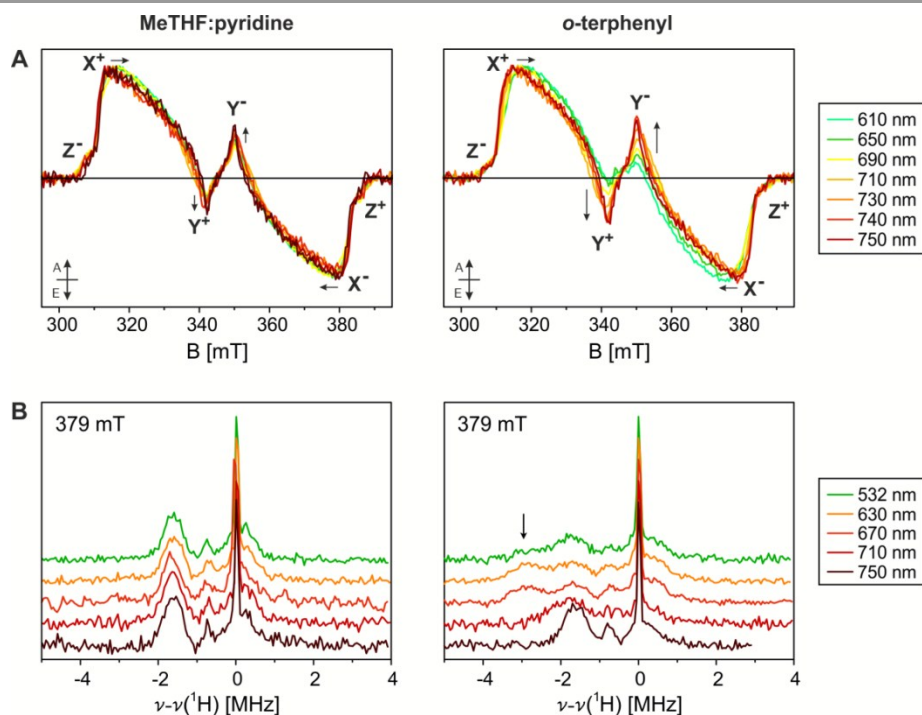
Figure 2. (A) Transient EPR spectra recorded at 20 K for **P2** in MeTHF:pyridine 10:1 (left) and in *o*-terphenyl (right) using different excitation wavelengths. The graphs shown were obtained as follows: EPR spectra were recorded using light polarized parallel, $I_\parallel$, or perpendicular, $I_\perp$, to the magnetic field and averaged up to 2 μs after the laser pulse. The depolarized spectra were then reconstructed as $\frac{1}{3}(I_\parallel + 2I_\perp)$ and normalized to the maximum. The direction of changes with increasing excitation wavelengths are indicated by arrows. (A=absorption, E=emission) (B) Mims ENDOR spectra recorded at 20 K at a magnetic field of 379 mT (high field X transition) for **P2** in MeTHF:pyridine 10:1 (left) and in *o*-terphenyl (right) using different excitation wavelengths. The arrow indicates the position of an additional ENDOR peak appearing for excitation at wavelengths ranging from 630 to 670 nm.
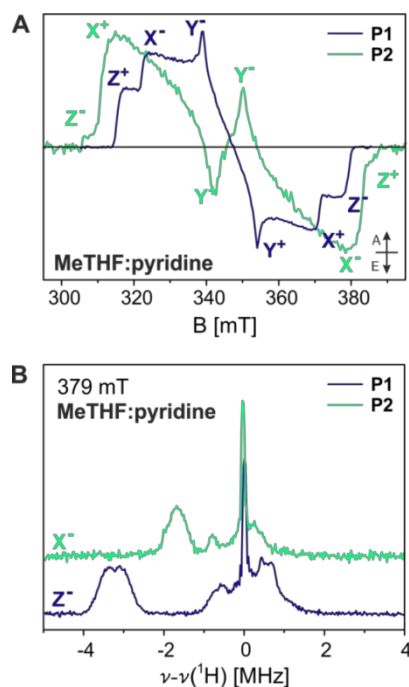

Figure 3. (A) Transient EPR spectra of **P1** and **P2** recorded at 20 K in MeTHF:pyridine 10:1 after excitation with depolarized laser light at 645 and 750 nm, respectively. (A=absorption, E=emission) (B) Mims ENDOR spectra of **P1** and **P2** recorded at 20 K at a magnetic field of 379 mT (high field Z transition for **P1**, high field X transition for **P2**) in MeTHF:pyridine 10:1 after excitation with unpolarized light at 532 nm.[21]

The ENDOR results are a clear indication of the localization of the triplet state on a single porphyrin unit for a perpendicular arrangement of the two porphyrin units in **P2**, although the changes observed in the transient EPR spectra at the same wavelengths are not straightforward to interpret. Attempts at reproducing the experimental EPR spectra as linear combinations of the planar dimer and monomer spectra have shown that the change in the intensity of the Y transitions and the shift of the X canonical peaks towards the centre of the spectrum can indeed be explained by the presence of a monomer-like contribution in the wavelength region from about 600 to 700 nm. The absence of additional peaks and the broadening of some of the features indicate the contribution of a distribution of different conformations characterized by different spectra, in agreement with the ENDOR results (see SI for a more detailed discussion and Figure S6).

Porphyrin trimer and tetramer

The porphyrin trimer and tetramer, **P3** and **P4**, can assume an even larger range of conformations as the torsional angles around the respectively two and three butadiyne links can now vary independently. The corresponding transient EPR spectra recorded in MeTHF:pyridine are shown in Figure 4. The wavelength-dependent changes are much more pronounced than in **P2** and occur to a similar degree in both MeTHF:pyridine and *o*-terphenyl (see Figure S7), suggesting
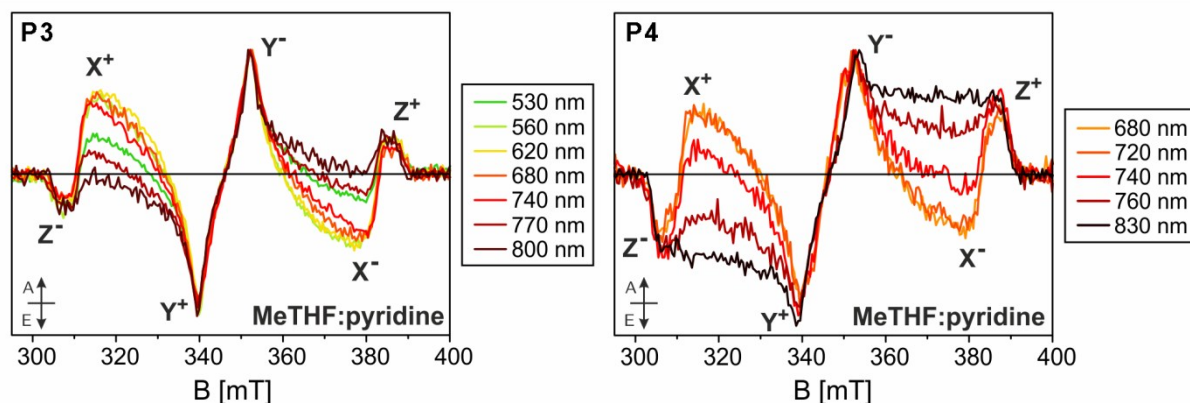
Figure 4. Transient EPR spectra recorded at 20 K for **P3** (left) and **P4** (right) in MeTHF:pyridine 10:1 using different excitation wavelengths. The spectra were recorded using light polarized parallel or perpendicular to the magnetic field and averaged up to 2 μs after the laser pulse and the depolarized spectra shown here were reconstructed as $\frac{1}{3}(I_\parallel + 2I_\perp)$. The spectra were normalized to the maximum.

that a wider range of conformations is present in both solvent systems. The changes in the EPR spectra are mainly restricted to the spin polarisation in the region of the X transitions, while the *D*-value and the relative intensities of the Y and Z transitions do not change. For **P3**, the intensity of the X transitions increases with excitation from 530 nm to higher wavelengths, reaches a maximum at about 620 nm and then decreases again. For **P4**, the maximum intensity is reached for a wavelength around 680 nm or lower and then decreases for longer wavelengths (Figure 4). At wavelengths higher than 800 nm for **P3** and higher than 830 nm for **P4** the intensity of the X transitions was found to increase again; no further changes are observed at even higher wavelengths before the signal intensity is reduced below the detection limit (data not shown). The exact nature of the contribution at high wavelengths could not be identified based on the available EPR data, but could be due to aggregation, which gives rise to absorptions at the red-end of the UV-vis–NIR spectrum in related systems and would therefore contribute most significantly to the EPR spectrum recorded in this region of the spectrum.[30] A small contribution of the aggregate spectrum at shorter wavelengths cannot be excluded, but based on the UV-vis-NIR data the main contribution to the signal is the free oligomer.

In analogy to the study of the wavelength dependence in the transient EPR spectrum of **P2**, an interpretation of the changes in the transient EPR spectra for **P3** and **P4** in terms of contribution of different twisted conformations was attempted. Since the completely planar conformation is characterized by the highest conjugation length,[4] the EPR spectra recorded close to the red-edge of the $S_0−S_1$ absorption band, at 800 nm for **P3** and at 830 nm for **P4**, were assigned to the approximately planar conformation of the oligomers. The corresponding ZFS parameters and relative sublevel populations are given in Table S1. The small changes in *D*-value observed for porphyrin oligomers with two or more porphyrin units, compared to the large change observed between **P1** and **P2**, has been attributed

to uneven spin density distributions in the longer oligomers, as confirmed by the hyperfine couplings obtained through ^{1}H ENDOR measurements.[22] The change in spin polarization between **P2** and the longer oligomers has been rationalized in terms of changes in the ISC mechanism, with an increasing contribution from Herzberg-Teller vibronic coupling which outweighs the direct Zn spin-orbit coupling contribution in the longer oligomers.[22]

A conformation with two coplanar porphyrin units can be expected to give a spectrum similar to that of the porphyrin dimer, which has similar *D*- and *E*-values to the trimer and tetramer, but a spin polarization characterized by a higher intensity of the X transitions and much lower intensities of the Y and Z transitions.[22] The contribution of such a spectrum to the planar **P3** or **P4** spectrum would lead to the observed wavelength-dependent changes, i.e. increased intensity of the X transitions in the region of the dimer absorption (approximately from 620 to 760 nm). The contribution of a conformation with all porphyrin units at right angles to each other is also likely and would resemble the EPR spectrum of **P1**. However, the analysis of the excitation wavelength dependence of **P2** has shown that the contribution of such a conformation is small compared to the coplanar conformation of the two porphyrin units and difficult to detect in the transient EPR spectra. Therefore, given the decreased signal-to-noise ratio of the experimental data recorded for **P3** and **P4**, a monomer-like contribution could not be distinguished from the dimer-like contribution with any confidence. Similarly, the presence of a contribution from a conformation with three coplanar porphyrin units and one unit at right angles in **P4** cannot be distinguished from a conformation with two coplanar porphyrin units due to the close similarity of the spin polarization of **P3** and **P4** spectra, essentially only differing in the intensity of the X transition.

The hypothesis of the contribution of a dimer-like spectrum for the twisted conformations is confirmed by subtraction of the **P3** or **P4** EPR spectrum obtained close to the red edge of the

absorption, assigned to the planar conformation, from the **P3** or **P4** spectra recorded at shorter wavelengths. The subtraction spectra correspond to the EPR spectra of the twisted conformations and closely resemble the **P2** EPR spectrum recorded at a wavelength around 710 nm (see Figure S8). Figure 5 shows that the wavelength-dependent EPR spectra of **P3** and **P4** can be obtained from the linear combination of the corresponding red edge spectrum and the dimer EPR spectrum (**P2**). The twisted conformations contribute mainly at
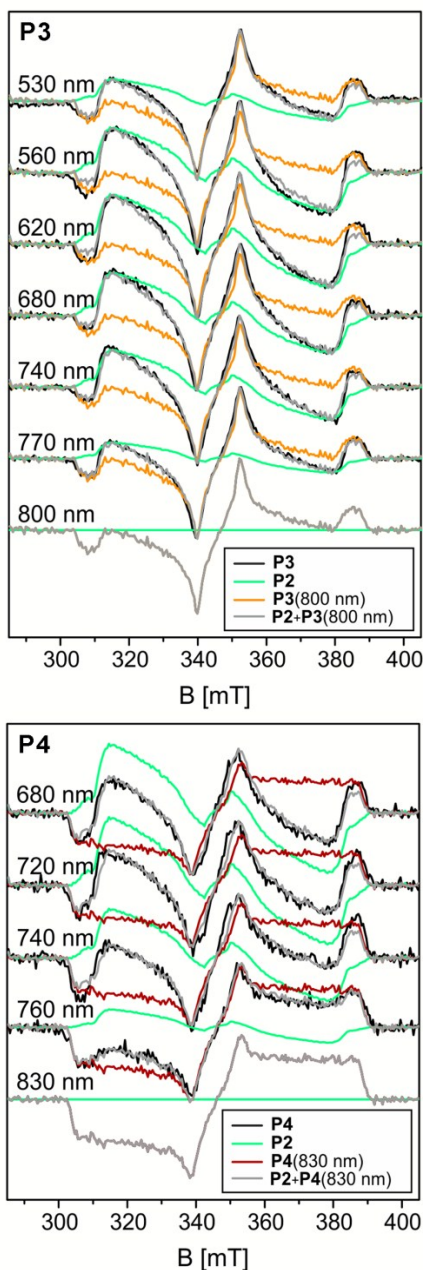

Figure 5. Reconstruction of the transient EPR spectra recorded for **P3** (top) and **P4** (bottom) at different wavelengths as a linear combination of the **P3**/**P4** spectrum recorded at 800/830 nm and the **P2** spectrum recorded in MeTHF:pyridine 10:1 with excitation at 710 nm.

wavelengths lower than 750 nm, in the region of the Q-band absorption of the porphyrin dimer.

Wavelength-dependent ENDOR for **P3** and **P4** was attempted, however the low triplet yield for these porphyrin oligomers, attributed to faster radiative and non-radiative decay of the singlet excited states,[31] prevented the measurement of spectra with a sufficiently high signal-to-noise ratio to allow their reliable interpretation.

Conclusions

In conclusion, this excitation wavelength-dependent EPR study has provided further insight into the effect of a conformational heterogeneity in porphyrin oligomers on triplet state delocalization. The changes observed in both EPR and ENDOR spectra of **P2** as a function of excitation wavelength can be explained by the contribution of different conformations with different dihedral angles between the two porphyrin units. By changing the excitation wavelength, only molecules in a planar conformation with an extensively delocalized triplet state or a mixture of molecules in a wider range of conformations with much more restricted distributions of the unpaired electrons can be selected. In addition to changes in the extent of triplet state delocalization, the two different conformations are also characterized by different spin alignments, reflected in the opposite sign of the zero-field splitting D parameter. Therefore the excitation wavelength dependence provides a certain degree of control over the spin properties of the triplet state, potentially relevant to applications in the field of spintronics.

An in-depth analysis and interpretation of the results for the porphyrin trimer and tetramer is complicated by the increased number of possible conformations and the lack of information on their contribution in different regions of the absorption spectrum. The changes in the transient EPR spectra can nevertheless be interpreted assuming two contributions: the contribution of a planar conformation with a spin polarization determined from the EPR spectrum recorded at the maximum of the Q-band absorption peak and the contribution of twisted conformations with a spin polarization similar to that of the porphyrin dimer. The observation of qualitatively similar results for the porphyrin trimer and tetramer indicates that similar effects occur in more extended systems, potentially covering a wider range of modulation of triplet state delocalization and therefore control over long-distance charge transport.

Acknowledgements

Notes and references

a Department of Chemistry, Centre for Advanced Electron Spin Resonance, University of Oxford, South Parks Road, Oxford OX1 3QR, UK.

b Department of Chemistry, Chemistry Research Laboratory, University of Oxford, 12 Mansfield Road, Oxford OX1 3TA, UK.

† Present address: Department of Chemistry, University of Washington, Seattle, WA 98195, USA.

1. H. L. Anderson, *Inorg. Chem.*, 1994, **33**, 972-981.

2. V. S.-Y. Lin, S. G. DiMagno and M. J. Therien, *Science*, 1994, **264**, 1105-1111.

3. J. Seth, V. Palaniappan, T. E. Johnson, S. Prathapan, J. S. Lindsey and D. F. Bocian, *J. Am. Chem. Soc.*, 1994, **116**, 10578-10592.

4. P. N. Taylor, J. Huuskonen, G. Rumbles, R. T. Aplin, E. Williams, H. L. Anderson, G. Rumbles and E. Williams, *Chem. Commun.*, 1998, **8**, 909-910.

5. R. Shediac, M. H. B. Gray, H. T. Uyeda, R. C. Johnson, J. T. Hupp, P. J. Angiolillo and M. J. Therien, *J. Am. Chem. Soc.*, 2000, **122**, 7017-7033.

6. H. S. Cho, D. H. Jeong, S. Cho, D. Kim, Y. Matsuzaki, K. Tanaka, A. Tsuda and A. Osuka, *J. Am. Chem. Soc.*, 2002, **124**, 14642-14654.

7. D. Holten, D. F. Bocian and J. S. Lindsey, *Acc. Chem. Res.*, 2002, **35**, 57-69.

8. D. Kim and A. Osuka, *Acc. Chem. Res.*, 2004, **37**, 735-745.

9. I.-W. Hwang, N. Aratani, A. Osuka and D. Kim, *Bull. Korean Chem. Soc.*, 2005, **26**, 19-31.

10. A. A. Kocherzhenko, S. Patwardhan, F. C. Grozema, H. L. Anderson and L. D. A. Siebbeles, *J. Am. Chem. Soc.*, 2009, **131**, 5522-5529.

11. G. Sedghi, V. M. García-Suárez, L. J. Esdaile, H. L. Anderson, C. J. Lambert, S. Martín, D. Bethell, S. J. Higgins, M. Elliott, N. Bennett, J. E. Macdonald and R. J. Nichols, *Nat. Nanotech.*, 2011, **6**, 517-523.

12. P. J. Angiolillo, V. S.-Y. Lin, J. M. Vanderkooi and M. J. Therien, *J. Am. Chem. Soc.*, 1995, **117**, 12514-12527.

13. J. Seth, V. Palaniappan, R. W. Wagner, T. E. Johnson, J. S. Lindsey and D. F. Bocian, *J. Am. Chem. Soc.*, 1996, **118**, 11194-11207.

14. D. Beljonne, G. E. O'Keefe, P. J. Hamer, R. H. Friend, H. L. Anderson and J. L. Brédas, *J. Chem. Phys.*, 1997, **106**, 9439-9460.

15. P. J. Angiolillo, K. Susumu, H. T. Uyeda, V. S.-Y. Lin, R. Shediac and M. J. Therien, *Synth. Metals*, 2001, **116**, 247-253.

16. D. Kim and A. Osuka, *J. Phys. Chem. A*, 2003, **107**, 8791-8816.

17. K. Susumu, P. R. Frail, P. J. Angiolillo and M. J. Therien, *J. Am. Chem. Soc.*, 2006, **128**, 8380-8381.

18. R. F. Kelley, M. J. Tauber and M. R. Wasielewski, *Angew. Chem. Int. Ed.*, 2006, **45**, 7979-7982.

19. M. U. Winters, E. Dahlstedt, H. E. Blades, C. J. Wilson, M. J. Frampton, H. L. Anderson and B. Albinsson, *J. Am. Chem. Soc.*, 2007, **129**, 4291-4297.

20. T. M. Wilson, T. Hori, M.-C. Yoon, N. Aratani, A. Osuka, D. Kim and M. R. Wasielewski, *J. Am. Chem. Soc.*, 2010, **132**, 1383-1388.

21. C. E. Tait, P. Neuhaus, H. L. Anderson and C. R. Timmel, *J. Am. Chem. Soc.*, 2015, **137**, 6670-6679.

22. C. E. Tait, P. Neuhaus, M. D. Peeks, H. L. Anderson and C. R. Timmel, *J. Am. Chem. Soc.*, 2015, **137**, 8284-8293.

23. A. R. Rocha, V. M. García-Suárez, S. W. Bailey, C. J. Lambert, J. Ferrer and S. Sanvito, *Nature Mat.*, 2005, **4**, 335-339.

24. P. J. Angiolillo, J. Rawson, P. R. Frail and M. J. Therien, *Chem. Commun.*, 2013, **49**, 9722-9724.

25. M. U. Winters, J. Kärnbratt, H. E. Blades, C. J. Wilson, M. J. Frampton, H. L. Anderson and B. Albinsson, *Chem. Eur. J.*, 2007, **13**, 7385-7394.

26. M. U. Winters, J. Kärnbratt, M. Eng, C. J. Wilson, H. L. Anderson and B. Albinsson, *J. Phys. Chem. C*, 2007, **111**, 7192-7199.

27. M. D. Peeks, P. Neuhaus and H. L. Anderson, *Phys. Chem. Chem. Phys.*, 2016, **18**, DOI: 10.1039/C1035CP06167x.

28. H. Xi, Y. Sun and L. Yu, *J. Chem. Phys.*, 2009, **130**, 094508.

29. M. K. Kuimova, M. Balaz, H. L. Anderson and P. R. Ogilby, *J. Am. Chem. Soc.*, 2009, **131**, 7948-7949.

30. J. Kärnbratt, M. Gilbert, J. K. Sprafke, H. L. Anderson and B. Albinsson, *J. Phys. Chem. C*, 2012, **116**, 19630-19635.

31. M. K. Kuimova, M. Hoffmann, M. U. Winters, M. Eng, M. Balaz, I. P. Clark, H. A. Collins, S. M. Tavender, C. J. Wilson, B. Albinsson, H. L. Anderson, A. W. Parker and D. Phillips, *Photochem. Photobiol. Sci.*, 2007, **6**, 675-682.

32. A. Richards, *University of Oxford Advanced Research Computing*, 2015, DOI: 10.5281/zenodo.22558.